Electronic Supplementary Information (ESI)

Water-soluble Conjugated Polyelectrolyte Brush Encapsulated Rare-earth Ion Doped Nanoparticles with Dual-upconversion Properties for Multicolor Cell Imaging

Wenbo Hu‡ [a], Xiaomei Lu‡[b], Rongcui Jiang[a], Quli Fan*[a], Hui Zhao[a], Weixing Deng[a], Lei Zhang[a], Ling Huang[b] and Wei Huang*[b]

Table of contents in Electronic Supplementary Information:

1. Experimental Section

Materials

$YCl_3.6H_2O$ (99.99%),$YbCl_3.6H_2O$ (99.99%),$ErCl_3.6H_2O$ (99.9%), NaOH (98%), NH4F (98%), 1-octadecene (90%) and oleic acid (90%) were purchased from Sigma-Aldrich and used as starting materials without further purification.

Synthesis of PFNBr

The water-soluble cationic conjugated polyelectrolyte brush (abbreviated as PFNBr, the chemical structures shown in Fig. 1) was synthesized by the previously reported method,[1, 2] which exhibits excellent water-solubility (28 mg mL^{-1}), much higher quantum yield (52%) and much higher stability in solution compared to other conjugated polyelectrolyte.

Synthesis of UCNPs

The oil-soluble UCNPs were synthesized according to a typical approach.[3, 4] The UCNPs was carried out following previous literature with slight modifications. 1 mmol of $RECl_3.H_2O$ (RE =Y^{3+}, Yb^{3+}, Er^{3+}) were added into a flask containing (50 mL) the mixture of 1-octadecene (ODE) and oleic acid (OA), at proper ratio according to the desired product phase and chemical composition. The solution was

heated to 160 ^{o}C for 30 min under argon protection and then cooled to room temperature. A methanol solution (10 mL) of NH_4F (1.6 mmol) and NaOH (1 mmol) were added to the flask and the resulting mixture was stirred for 30 min. After removal of the methanol and cyclohexane by evaporation, the solution was heated to 300 ^{o}C under an argon environment for 1 h and cooled to room temperature. The nanoparticles were precipitated by the addition of ethanol, collected by centrifugation, then washed with water and ethanol for several times, and finally dispersed in cyclohexane.

Synthesis of $NaYF_4$:Yb/Er@PFNBr nanocomposites

UCNPs was first dissolved in cyclohexane solution (2 mg/ml), followed by addition of PFNBr in water solution (1 mg/ml) with a certain ratio (cyclohexane : water = 100 μl : 5 ml) and emulsified for 2 min by pulsed sonication (50 W). The emulsion was then stirred at room temperature overnight to evaporate the organic solvent. The resulting nanocomposites were purified by high-speed centrifugation to remove excess PFNBr.

2. Instruments and characterization

The crystallographic information of the samples was obtained using XRD measurements, on a Bruker D8 Advance X-ray diffractometer with Cu Ka radiation (λ = 1.5406 Å) from 10 ^{o} to 80 ^{o} at a step of 5 ^{o}/min. Low resolution transmission electron microscopic (TEM) measurements were carried out using a JEOL JEM-2100 transmission electron microscope operating at an acceleration voltage of 100 kV. High resolution TEM (HRTEM) images were collected at a JEM-2100 transmission electron microscope. The nanoparticles were dispersed in water (1 wt %) in a standard quartz cuvette at room temperature to measure the photoluminescence spectra. The upconversion fluorescence spectra were collected on a Horiba JobinYvon FluoroMax-4 system and downconversion fluorescence spectra were collected on a Shimadzu RF-5301 PC spectrofluorometer using a 150 W xenon lamp as the excitation source. CLSM images were observed by confocal laser scanning microscope (Olympus, FV 1000).

Electronic Supplementary Information (ESI)

3.TEM, SEM, XRD, DLS characterization of $NaYF_4$:Yb/Er@PFNBr

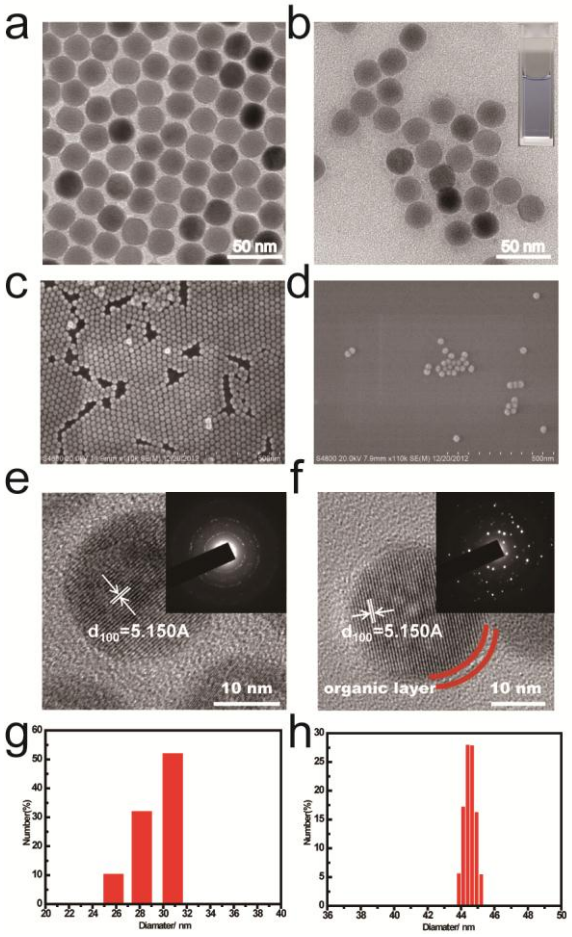

Fig.S1 a) TEM images of the nanoparticles before a) and after b) the encapsulation of PFNBr (the insert photograph is PFNBr encapsulated UCNPs soluble in aqueous solution). SEM images of the UCNPs before c) and after d) the encapsulation of PFNBr. HRTEM image of the UCNPs before e) and after f) the encapsulation of PFNBr, Inset SAED pattern of the UCNPs before and after the encapsulation of PFNBr. Hydrodynamic size distribution graphs of the UCNPs before g) and after h) the encapsulation of PFNBr.

The transmission electron microscopy (TEM) image in Fig.S1a and scanning electron microscope (SEM) image in Fig. S1c showed the synthesized $NaYF_4$:Yb/Er nanoparticles. All the $NaYF_4$:Yb/Er nanoparticles had regular and uniform sizes of ca. 29 nm. High-resolution TEM (HRTEM) images indicated that the interplanar spacing (d spacing) in nanoparticles before and after encapsulated with PFNBr was indexed as (100) lattice plane of hexagonal $NaYF_4$:Yb/Er with the value of 5.150A (Fig. S1e and f). The selected area electron diffraction (SAED) patterns in the insert of Fig. S1e and f were consistent with their HRTEM patterns. The crystallinity evolution of the nanoparticles before and after encapsulated with PFNBr could also be monitored by tracking the changes in the XRD patterns of the respective nanoparticles (Fig. S2a). All of the notable reflections in the XRD patterns can be perfectly assigned to those

calculated for the hexagonal $NaYF_4$:Yb/Er (JCPDS 16-0334). The nanocomposites retained the crystal structures of the original $NaYF_4$:Yb/Er nanoparticles, and thus their principal optical performances were also expected to be retained. Here we would like to emphasise that the crystal structure did not change after the encapsulation of PFNBr.

In the TEM images, only the core of $NaYF_4$:Yb/Er nanoparticles can be observed due to the lack of contrast between the organic shell and the background. But the encapsulated layer can be clearly observed as shown in the HRTEM which has drawn a red line (Fig. S1f). It was also worth noting that all the nanoparticles with single $NaYF_4$:Yb/Er cores well-dispersed in aqueous solution could also be observed clearly from Fig. S1b and their morphologies and sizes appeared similar to the pristine $NaYF_4$:Yb/Er. All of these indicated that the $NaYF_4$:Yb/Er cores were successfully encapsulated by PFNBr and no observed damage occurred during the process of encapsulation.

To fill the gaps of the weakness that the TEM images only provide information on the size of the $NaYF_4$:Yb/Er core, dynamic light scattering (DLS) measurements were carried out to further determine the hydrodynamic particle size of whole nanoparticles. The DLS measurements in Fig. S1g and 1h revealed that all the $NaYF_4$:Yb/Er nanoparticles encapsulated with PFNBr retained a relatively narrow size distribution with a mean size of around 44 nm, which is bigger than pure $NaYF_4$:Yb/Er core with a mean size of around 29 nm. These results showed that the encapsulation of PFNBr on the $NaYF_4$:Yb/Er surface did not influence the monodispersity of the $NaYF_4$:Yb/Er nanoparticles.

Electronic Supplementary Information (ESI)

4. XRD, Zeta Potentials characterization of $NaYF_4$:Yb/Er@PFNBr.

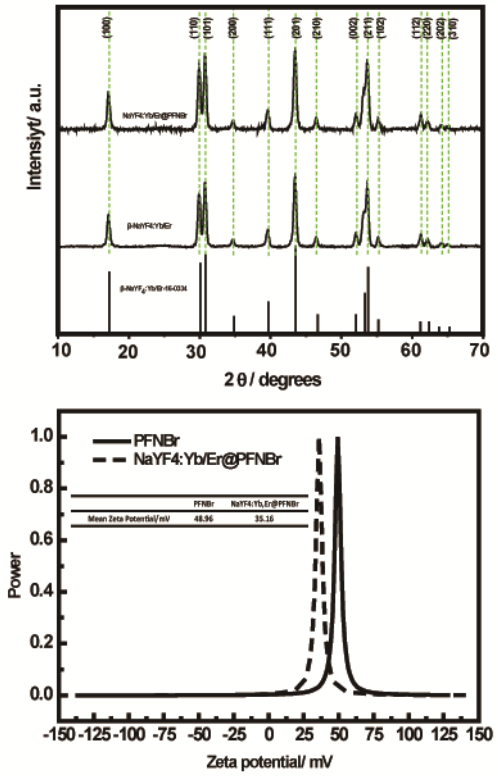

Fig.S2 a) XRD patterns of the UCNPs before and after the encapsulation of PFNBr. b) Zeta potentials of the PFNBr and NaYF4:Yb/Er@PFNBr.

The zeta potentials of the UCNPs encapsulated with PFNBr was further measured and showed in Fig.S2b. The zeta potentials of the pure PFNBr and $NaYF_4$:Yb/Er@PFNBr nanocomposites were +48.96 mV and +35.16mV, respectively. Such positive zeta potentials were generated from the protonation of the amine groups in aqueous solutions, indicating the successful encapsulation of the PFNBr on the nanoparticle surface.

Electronic Supplementary Information (ESI)

5. FTIR, TGA characterization of $NaYF_4$:Yb/Er@PFNBr.

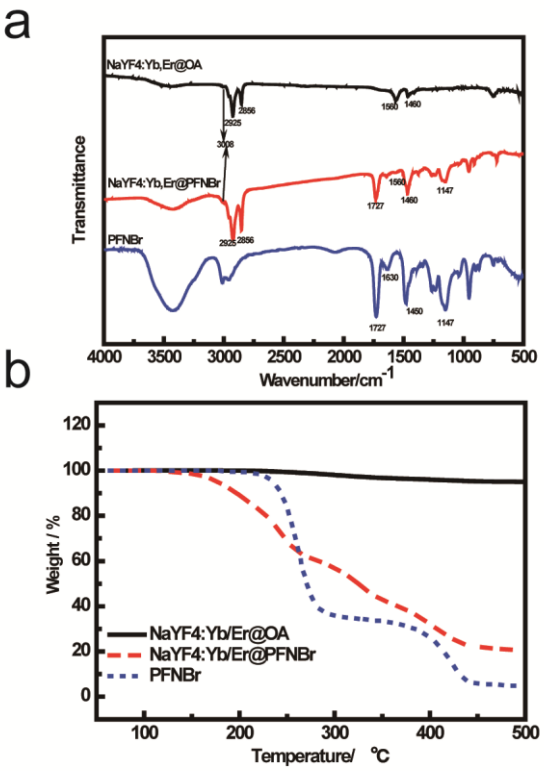

Fig. S3 a) FT-IR spectra of NaYF4:Yb/Er@OA, NaYF4:Yb/Er@PFNBr and PFNBr. b) TGA curves of NaYF4:Yb/Er@OA, NaYF4:Yb/Er@PFNBr and PFNBr.

To further confirm the UCNPs were encapsulated with PFNBr, The surface properties of the PFNBr, $NaYF_4$:Yb/Er@OA and $NaYF_4$:Yb/Er@PFNBr were investigated by Fourier transform infrared spectrometer (FTIR). As shown in Fig.S3a, the stretching vibrations of methylene in asymmetric C–H stretch at 2925 cm^{-1} and symmetric C–H stretch at 2856 cm^{-1} of the long alkyl chain[12] was observed in both $NaYF_4$:Yb/Er@OA and $NaYF_4$:Yb/Er@PFNBr. A peak band at 3008 cm^{-1} corresponding to the =C–H stretching vibration can be seen in spectra of both $NaYF_4$:Yb/Er@OA and $NaYF_4$:Yb/Er@PFNBr indicating the OA ligands on the surface of NaYF4:Yb/Er@OA were encapsulated rather than exchange by PFNBr.[13] In addition, bands at 1560 and 1460 cm^{-1}, associated with the asymmetric (yas) and symmetric (ys) stretching vibrations of the carboxylic group of the bound OA ligands,[12] were also found in the spectra of both $NaYF_4$:Yb/Er@OA and NaYF4:Yb/Er@PFNBr. These findings not only confirm the presence of OA ligands in both samples but also suggest that OA on the surface of $NaYF_4$:Yb/Er@OA was

not exchanged by PFNBr. In the case of $NaYF_4$:Yb/Er@PFNBr, new bands at 1727 and 1147 cm^{-1} were observed which were associated with the C=O stretching vibrations and C-O stretching vibrations of the ester in PFNBr respectively. After comparison with the FTIR spectrum of the pure PFNBr, it can be safely deduced that encapsulation of the PFNBr on the surface of $NaYF_4$:Yb/Er@OA was successful.

Thermogravimetric analysis (TGA) was performed to evaluate the ligand content in $NaYF_4$:Yb/Er@PFNBr sample as shown in Fig.S3b. The TGA curve of the pristine UCNPs showed a weight loss of about 5 wt% after the UCNPs were heated to 230 °C which was the content of the OA ligands.[12] The TGA curve of the PFNBr showed two weight loss stages in the range of 200 to 450 °C. The first weight loss stage in the temperature range of 200-300 °C is due to the loss of the quaternized segment.[14] The second stage from 350 to 450 °C was attributed to the combustion of the rest organic groups in the samples.[15] Such weight loss ratio of first and second stage was 2:1 which was consistent with the molecular weight of PFNBr.[2] The TGA curve of $NaYF_4$:Yb/Er@PFNBr showed new decomposition profile that was derivative of the following constituents PFNBr and OA on the surface of UCNPs. Since the FT-IR results have indicated that PFNBr was successfully encapsulated on the OA-coated UCNPs surface, the first onset temperature of 100 °C could be attributed to associated water deriving from quaternized segment. The second onset temperature of 230 °C was due to the OA ligands and quaternized segment of PFNBr coated on the UCNPs. The third onset temperature of 350 °C was due to the combustion of the rest of PFNBr. Considering that the total weight loss of $NaYF_4$:Yb/Er@PFNBr was about 75 wt%, the weight of the OA ligands on the surface of $NaYF_4$:Yb/Er@PFNBr was calculated to account for 1.3 wt % of the total weight. So the content of PFNBr encapsulated on the $NaYF_4$:Yb/Er surface accounted for about 73.7 wt%, which can be chiefly estimated from the weight loss in the TGA results. This large proportion of PFNBr encapsulated on the UCNPs thus rendered these nanocomposites good water-solubility and stability.

Electronic Supplementary Information (ESI)

6. ln-ln plots characterization of $NaYF_4$:Yb/Er@PFNBr.

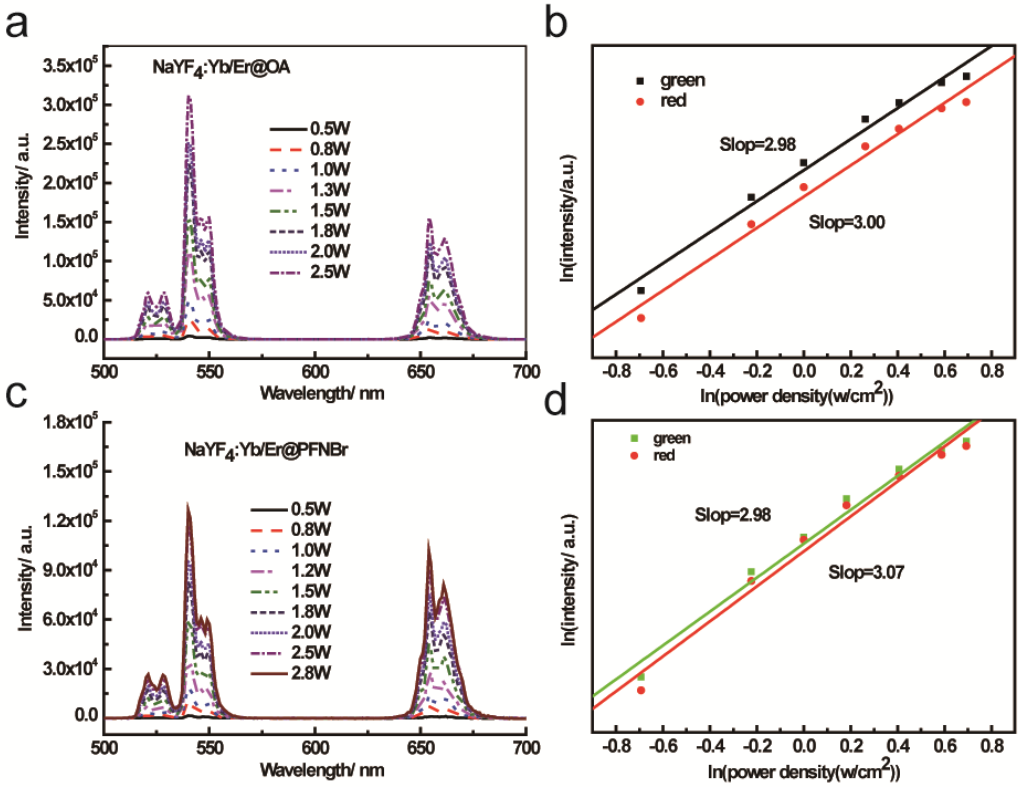

Fig.S4 The UCL intensity of the UCNPs before a) and after c) the encapsulation of PFNBr at different excitation power density. ln-ln diagrams of green and red luminescence intensities for the UCNPs before b) and after d) the encapsulation of PFNBr.

To further study the change about the intensity of red and green emission, the intensities of the UCL were recorded as a function of the 980 nm excitation intensity density in ln-ln plots (Fig.S4) to calculate the number of photons involved in the upconversion process.[16] Whether or not encapsulated both the slopes for the red emission curves are 2.98 while green emission curves are about 3.0 (Fig. S4b and d), indicating a three-photon emission process. This result suggested that aqueous solvent and the encapsulation of PFNBr did not have serious influence on the upconversion fluorescence which brings advantages in the application of biological imaging.

Electronic Supplementary Information (ESI)

7. In vitro cell viability of HepG-2 cells incubated with $NaYF_4$:Yb/Er@PFNBr

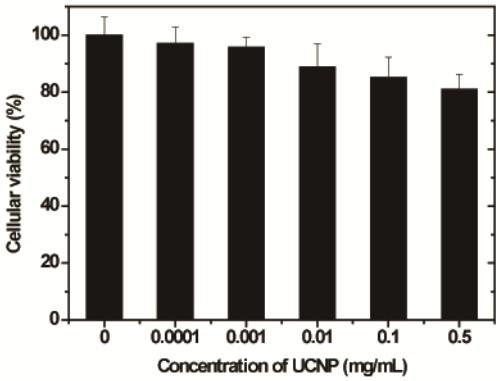

Fig.S5 In vitro cell viability of HepG-2 cells incubated with NaYF4:Yb/Er@PFNBr with different concentrations for 16 h at 37 ℃.

In order to validate the feasibility of $NaYF_4$:Yb/Er@PFNBr as biological probe and contrast medium in biological application, water-soluble $NaYF_4$:Yb/Er@PFNBr nanocomposites incubated with HepG-2 cells were chosen to be tested for cytotoxicity on the basis of the reduction activity of [3-(4,5-dimethylthiazol-2-yl)-2,5-diphenyltetrazolium bromide] (MTT). The viability of untreated cells as a control experiment was assumed to be 100%. No significant differences in the proliferation of the cells were observed in the absence or presence of UCNPs (Fig.S5). The cellular viabilities were estimated to be greater than 90% after 16 h. These data show that $NaYF_4$:Yb/Er@PFNBr nanocomposites can be considered to serve as a potential probe for luminescence imaging duo to the low cytotoxicity.

Electronic Supplementary Information (ESI)

8. Stability of $NaYF_4$:Yb/Er@PFNBr nanocomposites in PBS and serum.

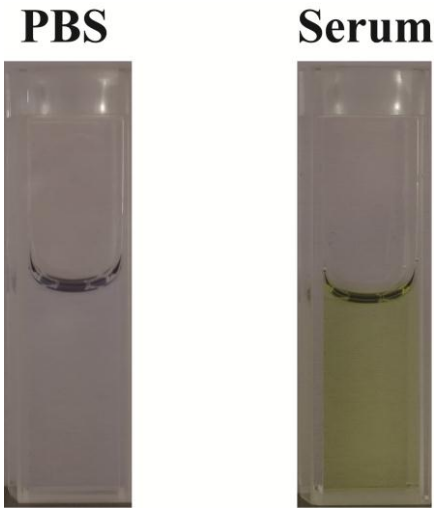

Fig.S6 Photos of $NaYF_4$:Yb/Er@PFNBr nanocomposites in PBS and serum solutions recorded after centrifugation at 6000rpm for 5 min (Hyclone was diluted in PBS to prepare serum soulution). No obvious precipitation was observed suggesting the good stability in PBS and serum.

9. Signal co-localization of HepG-2 cells incubated with $NaYF_4$:Yb/Er@PFNBr

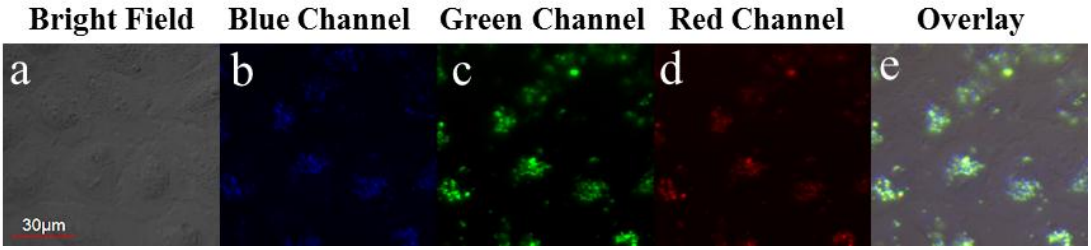

Fig.S7 In vitro cell experiments of the $NaYF_4$:Yb/Er@PFNBr nanocomposites under b) 800 nm irradiation and c, d) 980 nm irradiation. The overlay picture is a prefect demonstration of signal co-localization.

Electronic Supplementary Information (ESI)

References

1. Z. Zhang, Q. Fan, P. Sun, L. Liu, X. Lu, B. Li, Y. Quan and W. Huang, *Macromol. Rapid Commun.*, 2010, **31**, 2160-2165.
2. Z. Y. Zhang, X. M. Lu, Q. L. Fan, W. B. Hu and W. Huang, *Polym Chem*, 2011, **2**, 2369-2377.
3. X. Teng, Y. Zhu, W. Wei, S. Wang, J. Huang, R. Naccache, W. Hu, A. I. Tok, Y. Han, Q. Zhang, Q. Fan, W. Huang, J. A. Capobianco and L. Huang, *J. Am. Chem. Soc.*, 2012, **134**, 8340-8343.
4. F. Wang, Y. Han, C. S. Lim, Y. Lu, J. Wang, J. Xu, H. Chen, C. Zhang, M. Hong and X. Liu, *Nature*, 2010, **463**, 1061-1065.
5. C. Boyer, M. R. Whittaker, V. Bulmus, J. Liu and T. P. Davis, *NPG Asia Mater*, 2010, **2**, 23-30.
6. W. W. Yu, E. Chang, J. C. Falkner, J. Zhang, A. M. Al-Somali, C. M. Sayes, J. Johns, R. Drezek and V. L. Colvin, *J. Am. Chem. Soc.*, 2007, **129**, 2871-2879.
7. Y. Kang and T. A. Taton, *Angew. Chem., Int. Ed.*, 2005, **44**, 409-412.
8. Y. Wang, J. F. Wong, X. Teng, X. Z. Lin and H. Yang, *Nano Lett.*, 2003, **3**, 1555-1559.
9. B. Dubertret, P. Skourides, D. J. Norris, V. Noireaux, A. H. Brivanlou and A. Libchaber, *Science*, 2002, **298**, 1759-1762.
10. B.S. Kim, J.M. Qiu, J.P. Wang and T. A. Taton, *Nano Lett.*, 2005, **5**, 1987-1991.
11. T. Pellegrino, L. Manna, S. Kudera, T. Liedl, D. Koktysh, A. L. Rogach, S. Keller, J. Rädler, G. Natile and W. J. Parak, *Nano Lett.*, 2004, **4**, 703-707.
12. Z. Chen, H. Chen, H. Hu, M. Yu, F. Li, Q. Zhang, Z. Zhou, T. Yi and C. Huang, *J. Am. Chem. Soc.*, 2008, **130**, 3023-3029.
13. N. Bogdan, F. Vetrone, R. Roy and J. A. Capobianco, *J. Mater. Chem.*, 2010, **20**, 7543.
14. Q.L. Fan, S. Lu, Y.H. Lai, X.Y. Hou and W. Huang, *Macromolecules*, 2003, **36**, 6976-6984.
15. A. Midya, V. Mamidala, J. X. Yang, P. K. Ang, Z. K. Chen, W. Ji and K. P. Loh, *Small*, 2010, **6**, 2292-2300.
16. H.X. Mai, Y.W. Zhang, L.D. Sun and C.H. Yan, *J. Phys. Chem. C*, 2007, **111**, 13721-13729.